Environmental changes at the Frasnian–Famennian boundary in Central Morocco (Northern Gondwana): integrated rock-magnetic and geochemical studies

L. RIQUIER[1], O. AVERBUCH[1], N. TRIBOVILLARD[1], A. EL ALBANI[2], N. LAZREQ[3] & S. CHAKIRI[4]

[1]*UMR 8110, Processus et Bilans en Domaines Sédimentaires, Bâtiment SN5, Université de Lille 1, F-59655 Villeneuve d'Ascq cedex, France (e-mail: Laurent.Riquier@univ-lille1.fr)*

[2]*UMR 6532, Hydrogéologie, Argiles, Sols et Altérations, Bâtiment Sciences Naturelles, Université de Poitiers, 40 Avenue du recteur Pineau, F-86088 Poitiers cedex, France*

[3]*Université Cadi Ayyad de Marrakech, Faculté des Sciences Semlalia, Département de Géologie, Avenue du Prince Moulay Abdellah, BP 2390, 40001 Marrakech, Morocco*

[4]*Université Ibn Tofail, Faculté des Sciences, Laboratoire de Géologie dynamique et appliquée, BP 133, 14000 Kénitra, Morocco*

Abstract: Rock magnetic (magnetic susceptibility and hysteresis parameters) and geochemical analyses (major and trace elements) were carried out on whole rock samples of two Frasnian–Famennian boundary sections, Anajdam and Bou-Ounebdou in the Central Morocco (Western Meseta). During the Frasnian, the decreasing trend of the magnetic susceptibility signal, mainly carried by low-coercivity magnetite grains, indicates a gradual reduction of detrital influx. This decrease in detrital input parallels a Frasnian long-term sea-level rise. In the Late Frasnian Kellwasser Horizons, that are classically considered to represent highstand deposits, the magnetic signal exhibits the lowest intensities in connection with maximum diamagnetic contribution of the carbonate fraction. With respect to geochemical data, the two black carbonate-rich Kellwasser Horizons are characterized by noticeable positive anomalies of bottom-water dysoxic proxies and of marine primary productivity markers. Our data thus suggest that in Central Morocco, the Late Frasnian marine environments were marked by a relatively important biogenic productivity favouring the onset of oxygen-depleted conditions during periods of maximum transgression on the continental platforms.

The Frasnian–Famennian (F–F) boundary (Late Devonian, 374.5 Ma ago; Gradstein *et al.* 2004); was a major period of biodiversity loss and environmental changes. This boundary corresponds to one of the five biggest biological mass extinctions of the Phanerozoic, in which many species of marine organisms died out (e.g. corals, stromatoporoids, trilobites, conodonts, cephalopods) (Sepkoski 1982, 1986; Copper 1986; Sandberg *et al.* 1988; Schindler 1990; Becker & House 1994; McGhee 1996; Walliser 1996; Hallam & Wignall 1999; House 2002; Ma & Bai 2002; Racki *et al.* 2002). This period has been also suggested to be the time of significant climatic variations, attested by the $\delta^{18}O$ signature of marine conodonts apatite (Joachimski & Buggisch 2002; Joachimski *et al.* 2004) and the evolution of the miospore diversity on continents (Streel *et al.* 2000). Such climatic effects are likely to have induced global sea-level fluctuations that, combined with the changes in the erosional processes on land, potentially resulted in varying the intensity of the basinal detrital supply (e.g. Ellwood *et al.* 2000).

On the other hand, the Upper Frasnian interval is generally associated with the deposition of one or two organic-rich units in outer shelf and epicontinental basin settings, i.e. the Kellwasser (KW) Horizons (e.g. Buggisch & Clausen 1972; Sandberg *et al.* 1988; Schindler 1990; Buggisch 1991; Wendt & Belka 1991; Becker & House 1994). These beds have been recognized in many sections, located on the borders of Laurassian (N. America, N. Europe), Gondwanan (S. Europe, Africa), South China and on the southern border of the Siberian continents. Numerous factors controlling the KW organic-rich sediment accumulations have been proposed, such as increased primary productivity or bottom-water oxygen-depleted

From: BECKER, R. T. & KIRCHGASSER, W. T. (eds) *Devonian Events and Correlations*. Geological Society, London, Special Publications, **278**, 197–217. DOI: 10.1144/SP278.9
0305-8719/07/$15 © The Geological Society of London 2007.

conditions (e.g. Buggisch 1991; Joachimski & Buggisch 1993; Becker & House 1994; Murphy *et al.* 2000*a*, *b*; Bond *et al.* 2004; Tribovillard *et al.* 2004*a*; Riquier *et al.* 2005). These factors have been connected to different driving mechanisms acting in isolation or combined, such as sea-level fluctuations, climatic variations, land plants spreading, volcanism or mountain building (e.g. Becker & House 1994; Algeo & Scheckler 1998; Racki 1998, 1999; Joachimski & Buggisch 2002; Godderis & Joachimski 2004; Averbuch *et al.* 2005).

The aims of this study are to present the sedimentary record of the Late Devonian events from two Moroccan sections, where the KW horizons are particularly well exposed. Rock magnetic data, combined with clay mineralogical studies and geochemical analyses of major compounds, will be discussed with respect to the nature and the intensity of the detrital supply versus carbonate productivity during the F–F boundary events. An additional extensive geochemical data set of inorganic elemental ratios is presented here to document marine oxygen (O_2) levels and productivity conditions during deposition of the KW horizons.

Geological setting

The Central Moroccan Meseta belongs to the Variscan orogenic belt of Northern Africa (Fig. 1a). In Devonian times, it represents a transitional zone between platform domains to the west and southwest (Western Meseta) and a deep turbiditic basin to the east and north (Eastern Meseta, Rif; e.g. El Hassani & Tahiri 2000*a*; Chakiri 2002). This strongly segmented continental margin, which developed at subtropical palaeolatitudes along the northern border of Gondwana, was sequentially dismembered by thrust movements from Late Devonian (the internal metamorphic zones of the Eastern Meseta) to Upper Carboniferous times (the external non-metamorphic Central and Western Meseta; Bouabdelli 1989; Piqué *et al.* 1993; Bouabdelli & Piqué 1996).

In more detail, the two investigated sections, Bou-Ounebdou and Anajdam, were deposited in the Azrou–Kenifra Basin, which forms the easternmost termination of the Moroccan Central Massif. It developed as a transtensional basin in Lower Devonian times and was inverted not earlier than in Upper Viséan times as the thrust front propagated towards the southwest (Bouabdelli 1989). Both Upper Devonian sections, located in the M'rirt area (Fig. 1b), were thus deposited in a relatively tectonically quiet passive margin-type environment.

The sections of Bou-Ounebdou and Anajdam were well-studied Late Devonian sections: during the last decade, detailed investigations on sedimentary sequences and stratigraphy have been done, particularly within the IGCP projects 421 on 'North Gondwanan Mid-Palaeozoic bioevent/biogeography patterns in relation to crustal dynamics' (El Hassani & Tahiri 2000*a*) and by the Subcommission on Devonian Stratigraphy. The Anajdam and Bou-Ounebdou sections were described in detail by Lazreq (1992, 1999), Becker and House (2000), Walliser *et al.* (2000) and Chakiri (2002). The Bou-Ounebdou section has also been studied by Girard and Albarède (1996), Feist (2002) and Joachimski *et al.* (2002).

Bou-Ounebdou

The Bou-Ounebdou section, corresponding to the section M'rirt II in Walliser *et al.* (2000), is located in the M'rirt Nappe, about 5 km southeast of M'rirt (Fig. 1b). The sampled interval records condensed carbonate sedimentation from the Frasnian Lower *hassi* Zone to the Famennian Upper *triangularis* Zone (Fig. 2). The Late Devonian sequence is about 5.5 m thick and exposes a succession of cephalopod limestone beds, mudstones to wackestones in texture, with intercalated calcareous shale levels. The occurrence of pelagic and nektobenthic faunas argues for a moderately deep outer platform setting (Becker 1993; Becker & House 2000; Chakiri 2002). Two black limestone levels, which are globally time-equivalent to the KW horizons of the Rhenohercynian Massif (Germany), have been identified (Lazreq 1992; Becker 1993). The Lower Kellwasser (LKW) horizon is about 25 cm thick and is observed at the base of the Upper *rhenana* Zone. The 20 cm thick Upper Kellwasser Horizon (UKW) consists of lenticular lenses of black limestones, alternating with black shales. The two KW horizons contain abundant nektonic and planktonic fauna, including orthoconic nautiloids and ammonoids, conodonts and tentaculitids. Previously, the base of the UKW horizon was assigned to the uppermost part of the Upper *rhenana* Zone whereas the end of the UKW horizon was regarded as in the *linguiformis* Zone (Lazreq 1992, 1999). New biostratigraphical data from Becker & House (2000) and Girard *et al.* (2005) refined this stratigraphical framework showing that the UKW horizon was only restricted to the *linguiformis* Zone (Fig. 2). On top of the UKW horizon, the F–F boundary is represented by a surface of discontinuity (Lazreq 1999; Becker & House 2000; Chakiri 2002). Based on micro- and biofacies analysis, this discontinuity has been interpreted as the result of a significant sea-level fall (Chakiri 2002). However, the

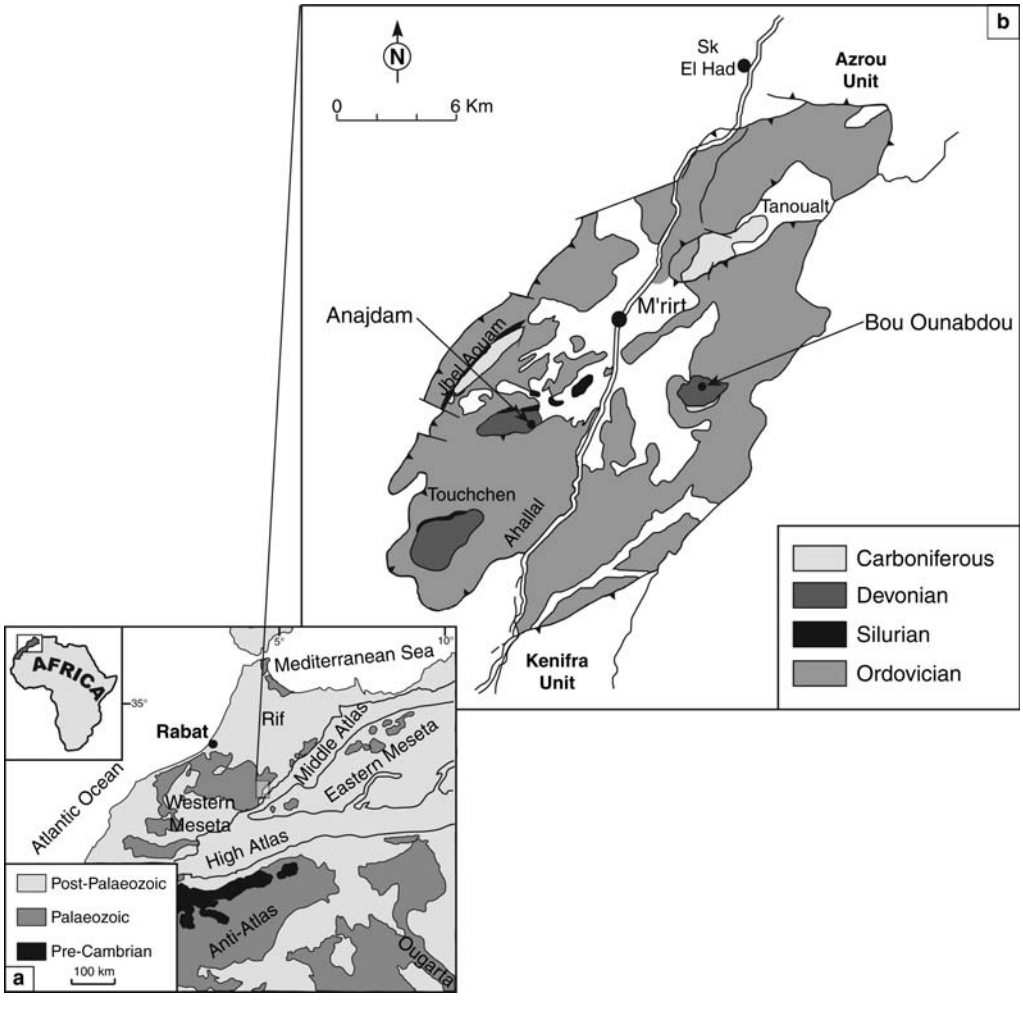

Fig. 1. (**a**) Main structural subdivision of middle and northern Morocco and (**b**) location of the studied sections in the M'rirt unit (modified from Bouabdelli 1989).

regression does not appear to have caused a zonal gap at the base of the Famennian (i.e. *triangularis* Zone), as illustrated by the correlation of the *Phoenixites* limestone (Lower *triangularis* Zone) observed between the M'rirt area and the Mont Peyroux Nappe (Montagne Noire) (Becker & House 2000). The sampled Lower Famennian deposits are characterized by 2 m thick, grey griotte limestones.

Anajdam

This section is located in a thrust-sheet developed in the footwall of the M'rirt nappe (Fig. 1b; Bouabdelli 1989). The exposed Upper Devonian succession is about 4.5 m thick and consists of bioclastic limestones with rare marly beds (Fig. 2). Limestone microfacies are represented mostly by packstones and wackestones. The investigated sequence begins within the *falsiovalis* Zone, at the Givetian–Frasnian boundary, and ranges up to the Lower *triangularis* Zone in basal Famennian times (Lazreq 1999). The faunal associations (conodonts, ammonoids, ostracodes and gastropods) characterize an external platform setting. In the Late Frasnian, two 20–45 cm thick dark-grey and black limestone horizons were biostratigraphically identified as the LKW horizon at the base of the Upper *rhenana* Zone, and the UKW horizon, within the *linguiformis* Zone (Fig. 2).

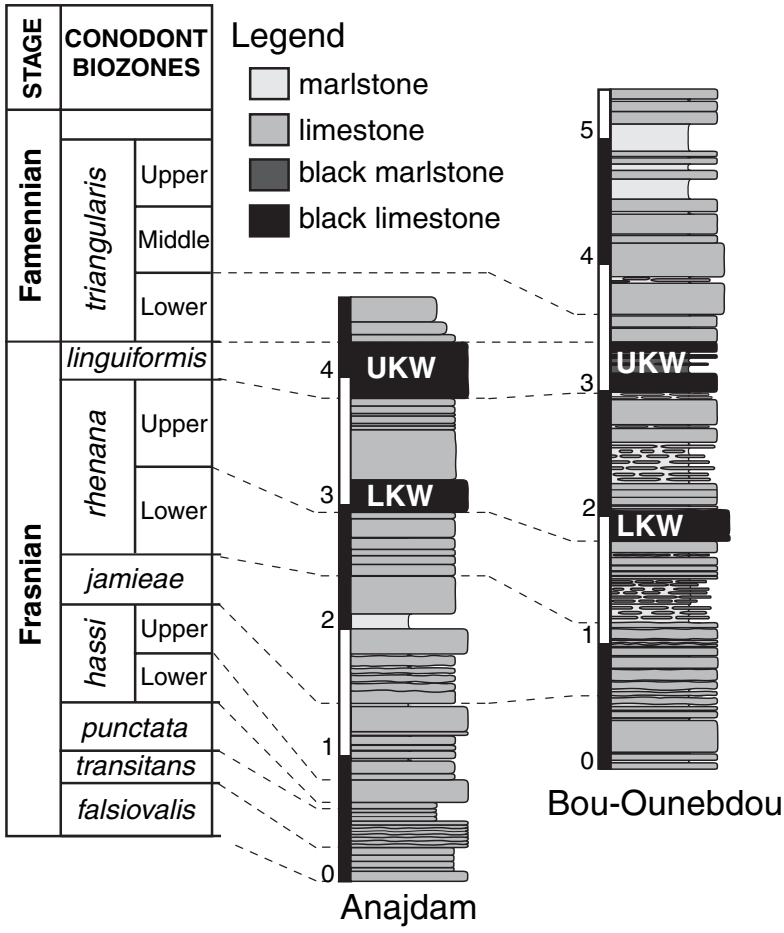

Fig. 2. Stratigraphical columns of the Frasnian–Famennian boundary beds in Anajdam and Bou-Ounebdou (biostratigraphical correlation based on data from Lazreq 1999; Becker & House 2000; Girard *et al.* 2005).

Material and analytical methods

Clay mineralogy

Clay mineral associations have been investigated by X-ray diffraction (XRD) using oriented mounts of the <2 μm size fraction containing non-calcareous particles. Deflocculation of clay aggregates was performed by successive washing with distilled water after decarbonatation of the crushed rock samples. The clay-sized fraction (<2 μm) was separated by settling and centrifugation and placed onto two glass slides and left dry in order to prepare oriented specimens. One of the air-dried, oriented clay-aggregate mounts was saturated in an ethylene glycol atmosphere at 20 °C overnight and another one was heated for two hours at 490 °C (Holtzapffel 1985). So, a series of three X-ray diffractograms was performed for each sample after air-drying, ethylene-glycol solvation and heating. X-ray diffractograms were obtained using a Philips PW 1729 diffractometer, with CuKα radiations and Ni filter, operating at a voltage of 40 KV and a current of 25 mA at a scanning rate of $1°2\theta/\text{min}$.

The identification of clay minerals was made according to the position of the (001) series of basal reflections on the three X-ray diffractograms (Brindley & Brown 1980). Semi-quantitative estimations of major clay minerals, as well as the illite crystallinity index, have been calculated using the Macdiff software (Petschick *et al.* 1996). Measured illite crystallinity index values were converted into the international calibrated scale CIS (Warr & Rice 1994) using a routine correlation process exposed in Robion *et al.* (1999).

The reproducibility of technical works and measurements was tested: the relative error is 5%.

Rock magnetism

The rock magnetic study integrated along-section magnetic susceptibility measurements coupled to representative measurements of magnetic hysteresis loops. The magnetic susceptibility quantifies the ability of the sedimentary rocks under study to be magnetized in a weak magnetic field, according to the respective concentrations of dia- (mainly calcite and quartz), para- (mainly illite, smectite, pyrite) and ferromagnetic *sensu lato* minerals (e.g. magnetite, goethite, haematite, pyrrhotite; see for example Walden *et al.* 1999 or Maher & Thompson 1999 for a more detailed description). In ancient sedimentary rocks, in the absence of intense diagenetic alteration, the magnetic susceptibility has been widely shown to provide a record of the bulk mineralogical changes induced by detrital inputs (magnetite, clays) and biogenic pelagic dilution (diamagnetic calcite; e.g. Crick *et al.* 1997; Devleeschouwer 1999; Ellwood *et al.* 2000; Tribovillard *et al.* 2002). The magnetic susceptibility data set includes 130 samples (70 measurements in Anajdam and 60 in Bou-Ounebdou) collected at 5 to 10 cm intervals, allowing high-resolution study of the magnetic susceptibility fluctuations. Low-field magnetic susceptibility was measured on small rock samples using a Kappabridge KLY-2 susceptibility bridge operating at an alternating-magnetic field of 300 A/m. Each sample was measured three times and a mean of these measurements is reported as the magnetic susceptibility value for that sample. Magnetic susceptibility values are normalized with respect to sample mass. Samples were weighted with a precision of 0.01 g from rock chips. So, results are reported here in mass-normalized magnetic susceptibility, hereafter χ ($m^3\ kg^{-1}$).

Hysteresis parameters were obtained from selected samples (15 measures for each section), using 10–30 mg chips, analysed at room temperature with an Alternating Gradient Force Magnetometer (AGFM 2900) at the Laboratoire des Sciences du Climat et de l'Environnement (Gif-sur-Yvette, France). By definition, hysteresis loops show the evolution of magnetization (M) of magnetic elements as a function of the applied magnetic field (H) (Fig. 3) (e.g. Borradaile *et al.* 1993; Walden *et al.* 1999). The sample is vibrated at room temperature in a magnetic field that is swept from 0 to +1 to −1 T then back to 0 T. From hystereris loop, four parameters are extracted: the saturation (isothermal) magnetization M_s ($\mu A.m^2$), the saturation (isothermal) remanent magnetization M_r ($\mu A.m^2$), the coercive force H_c (mT), and the coercivity of the remanence H_{cr} (mT) (Fig. 3). Values of M_s, M_r and H_c were determined for each hysteresis loop, after corrections for the high-field slope (SC: Slope Correction), which records the combined effects of paramagnetic and diamagnetic contributions. As for χ, magnetic parameters M_s, M_r and SC are normalized with respect to sample mass. H_{cr} was determined by stepwise application of a back-field isothermal remanence to remove the saturation remanence. The hysteresis parameters, described above, will be used here to discuss the origin of the magnetic susceptibility variations by characterizing (1) the relative contributions of the ferromagnetic versus para- or diamagnetic components and (2) the nature and amount of ferromagnetic minerals and especially of magnetite type, which can be generally used as a proxy of the detrital input (e.g. Borradaile *et al.* 1993; Vanderaveroet *et al.* 1999; Walden *et al.* 1999; Ellwood *et al.* 2000).

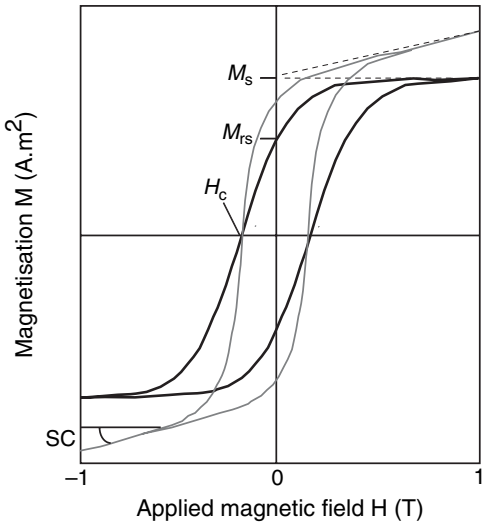

Fig. 3. Schematic hysteresis loop for a magnetite sample. The light grey loop is the original measurement, the black loop represents the same curve after corrections. The parameters saturation magnetization M_s, saturation remanent magnetization M_r, coercive force H_c, coercivity of remanence H_{cr} and slope correction SC are indicated.

Inorganic geochemistry

For each section, about 20 whole-rock geochemical analyses were made allowing the determination of major (Al, K, Si, Ti) and trace (Ba, Co, Cr, Cu, Mo, Ni, Th, U, V) elementary concentrations. Geochemical analyses were performed by ICP-AES (major or minor elements) and ICP-MS

(trace elements), at the spectrochemical laboratory of the Service d'Analyse des Roches et des Minéraux of the Centre National de la Recherche Scientifique (Vandœuvre-les-Nancy, France). The samples were prepared by fusion with $LiBO_2$ and HNO_3 dissolution. Precision and accuracy were both found to be better than 1% (mean 0.5%) for major-minor elements, 5% for Co, Cr, Mo, U and V and 10% for Cu, as checked by international standards and analysis of replicate samples, respectively. Carbonate content was determined using a Bernard calcimeter (acid digestion).

The trace-element concentrations were normalized to aluminium to avoid dilution effects by the carbonate fraction and to compare different environmental settings with regard to variations in trace-element contents. Higher element/Al ratios will indicate synsedimentary additions, if a constant composition of the background is assumed. Variations of the Al content in relation to diagenetic formation of clay minerals is unlikely, because in the present study, Al is positively correlated with Ti ($r^2 = 0.99$ for both sections) that is not incorporated during authigenic clay-mineral formation (Calvert & Pedersen 1993).

Results

Clay mineral analysis

X-ray diffraction analyses show that the clay assemblages in both sections are very close and dominantly composed of illite (about 80%) and chlorite (about 10%) (Fig. 4). Diagenesis-sensitive minerals, such as kaolinite or smectite, are either absent or present in traces suggesting a significant diagenetic imprint on the primary detrital clay assemblages. The data of Crystallinity Index Standard (CIS) of illite oscillate globally from 0.25 to 0.50 with an average value of 0.37 for the Bou-Ounebdou section and 0.41 for the Anajdam section (Fig. 4). According to the reference data from Warr & Rice (1994), these analyses indicate that both sections have been affected by a pronounced diagenesis, in the limit of the anchimetamorphic conditions. As a whole, these results are, however, in agreement with recent studies of colour alteration index (CAI) of conodont, suggesting that the maximum temperatures during thrust-related burial in the Central Moroccan Meseta did not exceed about 250 °C (Dopieralska 2003).

Rock-magnetic measurements

Magnetic susceptibility signal. Figure 5 shows the stratigraphical variations of the magnetic susceptibility and the $CaCO_3$ content for the two sedimentary sequences studied. As usually recorded in carbonate formation, the χ signal is broadly low ($<20.0 \times 10^{-8}\ m^3\ kg^{-1}$) but displays significant evolutions along sections, with short- and long-term variations.

Along the Anajdam section, the χ values mostly vary from 2.6 to $15.3 \times 10^{-8}\ m^3\ kg^{-1}$ with the exception of the two KW horizons. In these peculiar horizons, the χ values never exceed $1.5 \times 10^{-8}\ m^3\ kg^{-1}$. During the Frasnian, two successive slight and gradual decreasing trends, separated by a positive shift to values around $8.9 \times 10^{-8}\ m^3\ kg^{-1}$, are observed in the χ signal (Fig. 5). The first decreasing trend occurs from the base of the section (*falsovialis* Zone) up to the early part of the *jamieae* Zone, the second from the middle part of the *jamieae* Zone up to the base of the LKW horizon (Upper *rhenana* Zone). Within the LKW horizon, the χ record shows a sharp decrease to average values around $1.3 \times 10^{-8}\ m^3\ kg^{-1}$. The lowest χ value ($0.4 \times 10^{-8}\ m^3\ kg^{-1}$) is observed just above the LKW horizon. The inter-KW timespan is marked by a well-marked peak (up to the maximum χ value of $15.3 \times 10^{-8}\ m^3\ kg^{-1}$). The base of the UKW horizon displays a strong decrease of χ that remains of low values (around $1.3 \times 10^{-8}\ m^3\ kg^{-1}$) all along the UKW horizon. An increase of χ is recorded at the base of the Famennian times but its amplitude is difficult to resolve as sampling was not extended higher than the Lower *triangularis* Zone in basal Famennian times.

In the Bou-Ounebdou section, the χ values are about twice lower than those observed in the Anajdam section. They vary from 1.5 to $6.7 \times 10^{-8}\ m^3\ kg^{-1}$ with an interval of lowest values of $1.0 \times 10^{-8}\ m^3\ kg^{-1}$, measured in the LKW horizon (Fig. 5). From the base of the section up to the LKW level, the data are noisy and no clear trend is observed in the χ signal. Above the base of the LKW horizon, a comparable trend to Anajdam is observed with, however, a significant decrease in the amplitude of variations. The UKW horizon is marked by a slight decrease of χ values, following by a slight increasing trend toward average χ values of $3.0 \times 10^{-8}\ m^3\ kg^{-1}$ during the early Famennian.

The susceptibility data thus allow evidencing a contrast in the sedimentary record of both Moroccan sections. Unlike the more distal Bou-Ounebdou section, the samples of Anajdam exhibit well-defined variations of χ signal with particularly well-marked KW horizons. The trends point to a general long-term decrease during the Frasnian with minimum values localised within the two KW horizons. It is worth noting that these horizons display some significant increases in the carbonate content (up to 95–98%) but, by contrast, the

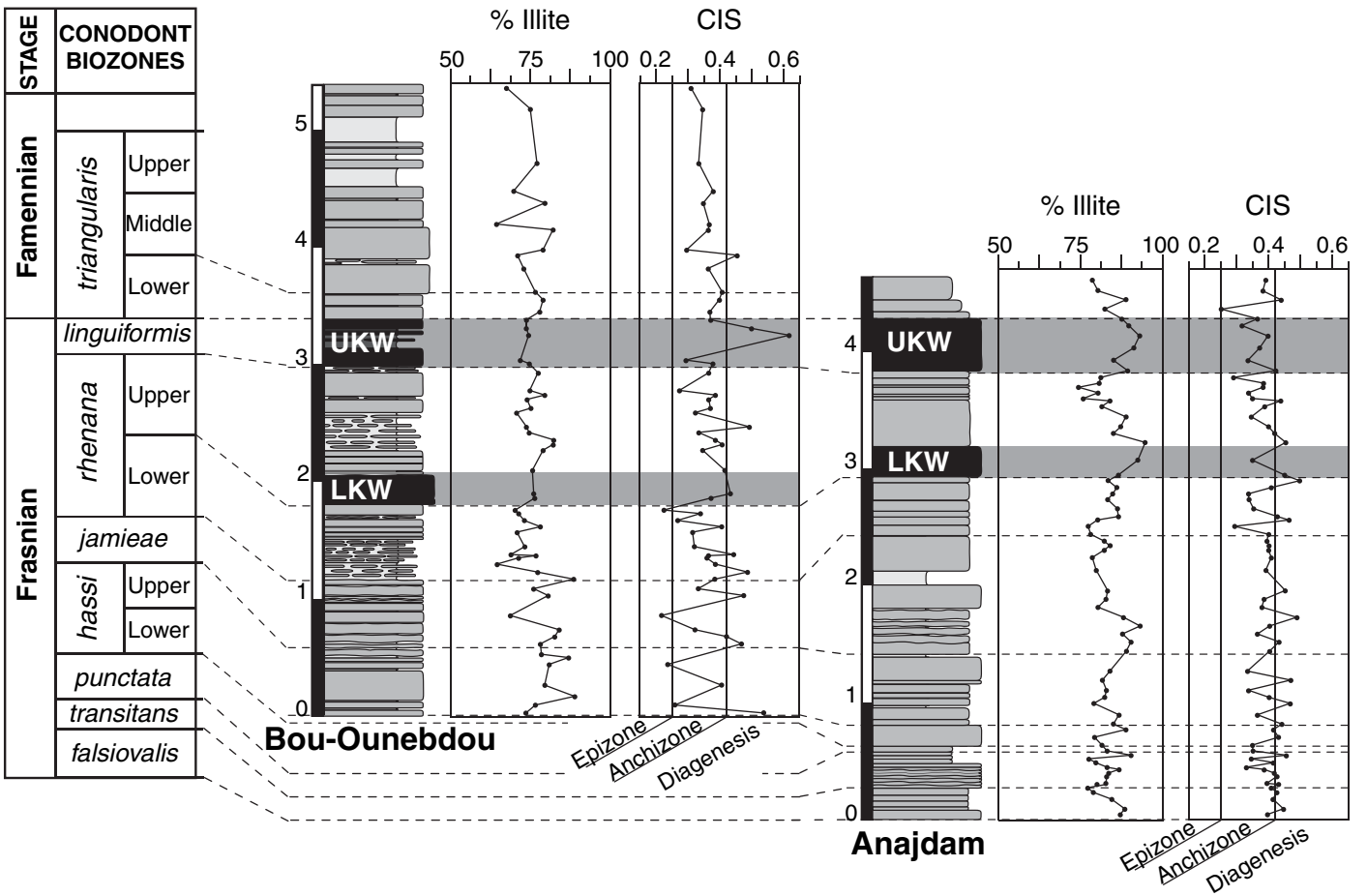

Fig. 4. Stratigraphical variation of percentage of illite and Crystallinity Index Standard of the sedimentary sequence from Bou-Ounebdou and Anajdam. Ranges for CIS are from Warr & Rice (1994).

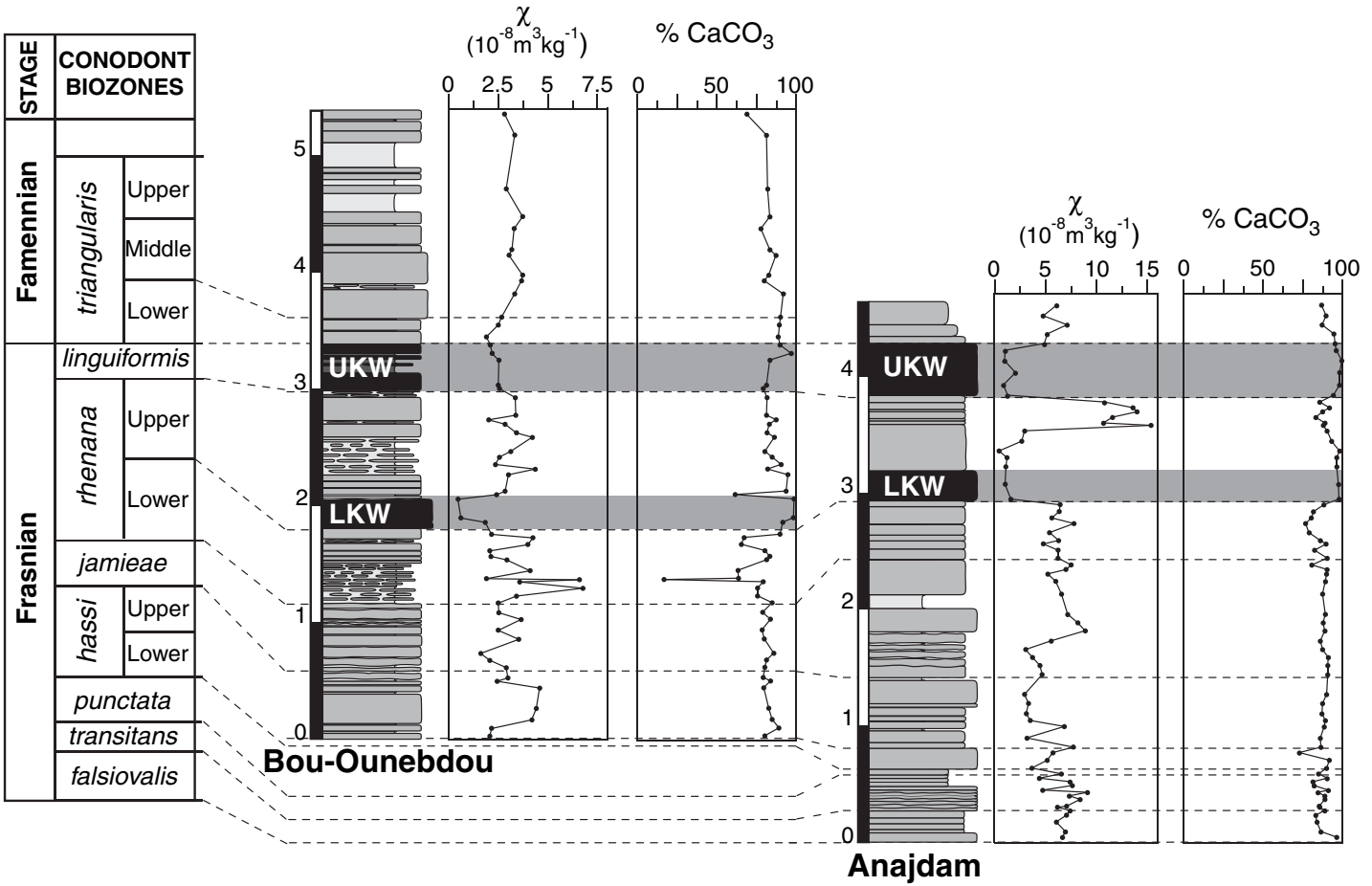

Fig. 5. Stratigraphical variation of mass-normalized magnetic susceptibility and calcium carbonate content of the sedimentary sequence from Bou-Ounebdou and Anajdam.

long-term χ decrease is not accompanied by noticeable variations of the carbonate content (Fig. 5). In both sections, the F-F boundary is marked by an increase in χ values of moderate amplitude.

Magnetic hysteresis properties. Magnetic hysteresis experiments have been carried out for representative samples of both sections (a total of 30 measurements) to provide information about the origin of the χ variations. Measured hysteresis parameters are plotted versus the magnetic susceptibility in Figure 6 to test the possible correlations existing between χ and the different hysteresis parameters.

As expected in carbonate rocks (e.g. Borradaile *et al.* 1993), values of M_s and M_r are globally low. In the Bou-Ounebdou section, as it was observed for χ, the amplitude of variation of M_s is also very low so that any convincing relationship can be drawn between these two parameters. Conversely, in Anajdam, an excellent correlation is observed between χ and M_s (Fig. 6a) thus indicating that the ferromagnetic *sensu lato* contribution controls the χ signal. The H_{cr} values are globally low in Anajdam (around 50 mT) regardless of the χ values (Fig. 6b) but they are significantly higher for much of the samples of Bou-Ounebdou ($60 \leq H_{cr} \leq 250$ mT). These data suggest that, in Anajdam, the χ variations are related to the varying concentration of a low coercivity mineral of magnetite type (Fe_3O_4) whereas, in Bou-Ounebdou, a mixture of magnetite and a higher coercivity phase is put forward. As usually observed in non-red limestone sequences, the latter is probably composed of low susceptibility goethite (FeO(OH); e.g. Heller 1978; Borradaile *et al.* 1993). This suggests an increase of the weathering intensity in the Bou-Ounebdou section compared to that of Anajdam, which is of crucial importance to recognize and understand the difference in the behaviour of iron-bearing minerals in both sections.

Samples with magnetite as the main carrier of the magnetic susceptibility ($H_{cr} < 70$ mT) have been plotted in a classical M_r/M_s versus H_{cr}/H_c graph (Fig. 7) in order to evaluate the bulk grain-size of the ferromagnetic fraction (Day *et al.* 1977). For both sections, the M_r/M_s ratio ranges from 0.1 to 0.25 and the H_{cr}/H_c ratio from 2 to 10. Following boundary values established by Dunlop (1986) and recommended by Borradaile *et al.* (1993), the diagram points to a dominant coarse-grain magnetic fraction with pseudo-single domain (PSD) to multi-domain (MD) behaviours although some points display a slight shift compared to the reference boundaries. Such shift has been observed in other magnetic hysteresis studies of carbonate rocks (e.g. Borradaile *et al.* 1993;

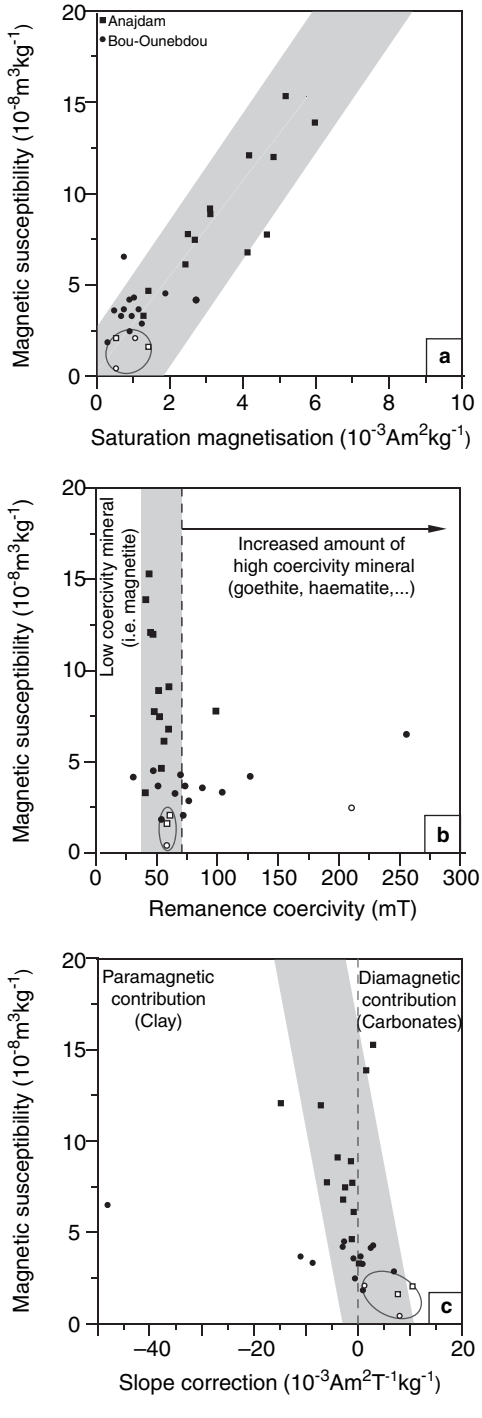

Fig. 6. Hysteresis parameters plotted against low-field mass susceptibility (χ) for representative samples from Anajdam and Bou-Ounebdou. (**a**) Saturation magnetization (M_s) *vs.* χ (**b**), coercivity (H_c) *vs.* χ and (**c**) Slope Correction *vs.* χ.

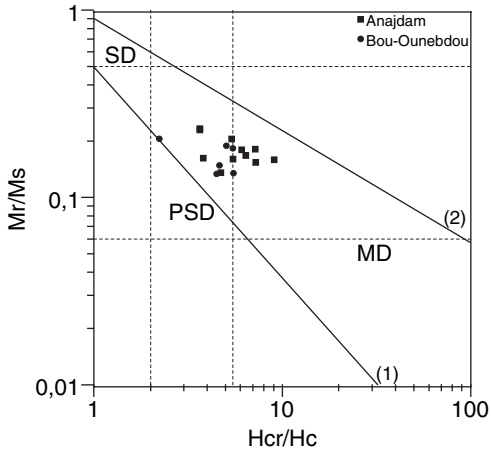

Fig. 7. Hysteresis parameters of samples from Anajdam and Bou-Ounebdou plotted according to Day *et al.* (1977). Ranges for *SD* (single domain), *PSD* (pseudo-single domain) and *MD* (multi-domain) are from Dunlop (1986). Empirical trends are shown for (1) unremagnetized and (2) remagnetized limestones (from Channell & McCabe 1994).

Katz *et al.* 2000) and, to our knowledge, has not yet received any satisfactory explanation. Furthermore, M_r/M_s and H_{cr}/H_c values cluster in between the lines established by Channell and McCabe (1994) for diagenesis-induced remagnetized limestones and non-remagnetized limestones (Fig. 7). This, at least, suggests that the primary depositional ferromagnetic signal has not been completely overprinted by diagenetic processes.

The paramagnetic and diamagnetic contributions, quantified by the high-field slope correction SC (Fig. 6c), display noticeable variations showing the varying respective amounts of iron-bearing clays (illites, chlorites) and carbonates. It clearly appears that the matrix of the limestones is diamagnetic in the KW horizons, whereas it is dominantly paramagnetic for the rest of the sedimentary record in both sections. A general anti-correlation of SC and χ is noticed, illustrating the relative increase of clay concentration in levels with high χ (Fig. 6c). Therefore, almost pure carbonates such as the KW levels display the highest diamagnetic contributions and the lowest χ values.

To summarize, hysteresis data thus demonstrate that the χ signal is controlled by the combined contributions of ferromagnetic *sensu lato* magnetite and paramagnetic clays. As shown in Figure 4, the diamagnetic contribution of calcite only exerts a noticeable control on magnetic susceptibility in the almost pure KW limestones. In Bou-Ounebdou, this pattern is perturbed by weathering processes which reduce the intensity and amplitude of variations of the χ signal by transforming high susceptibility magnetite into low susceptibility goethite. Therefore, the Bou-Ounebdou section cannot be considered as a reference sequence regarding the analysis of detrital input evolution in the F–F times in the M'rirt area. In the following, the discussion of the magnetic data will thus focus on the Anajdam section.

Inorganic geochemistry analysis

Figure 8 shows the stratigraphical evolutions of some Al-normalized elemental ratios, usually considered as reliable geochemical proxies to estimate the fluctuation of clastic fluxes as well as oxygenation and primary productivity levels in marine environments.

Clastic influx proxies. Some elements, including Ti, Si and K are considered to be indicators of detrital influx (Tribovillard *et al.* 1994; Murphy *et al.* 2000*b*). Titanium is usually associated with clay minerals and heavy minerals (ilmenite, rutile). Potassium occurs dominantly in clays, whereas Si occurs in both siliciclastic and biogenic fractions (e.g. quartz *vs.* opal). Normalized to Al, which only occurs in aluminosilicates, the Si, Ti and K ratios provide useful information about change in the contribution of elemental concentrations from detrital non-aluminosilicate sources.

In regard to clastic influx, Al-normalized Si, Ti and K concentrations do not show clear trends at the F–F boundary (Fig. 8). The KW horizons are not marked by noticeable increase or decrease of these elements. For both sections, the Ti/Al profile remains almost constant. The values are nearly around the average shale values of 0.053 (Wedepohl 1991) in the major part of the section whereas most of the samples from the KW horizons have a concentration of Ti below the detection limit. Concerning the evolution of the Si/Al ratio in the Anajdam section, the KW horizons are characterized by relatively lower values compared to the concentrations in the overlying and underlying strata. In Bou-Ounebdou, there is a relative stability of the Si/Al ratio during the Late Frasnian, followed by a gradual decrease in the Early Famennian. To some extent, the Si/Al curves show comparable trends for both studied sections. Finally, K/Al ratio is relatively stable; it records the highest values at the end of the two KW horizons (inputs of K-carrying minerals, such as illite-mica or K-feldspar) and the lowest values during the inter-KW timespan for both sections.

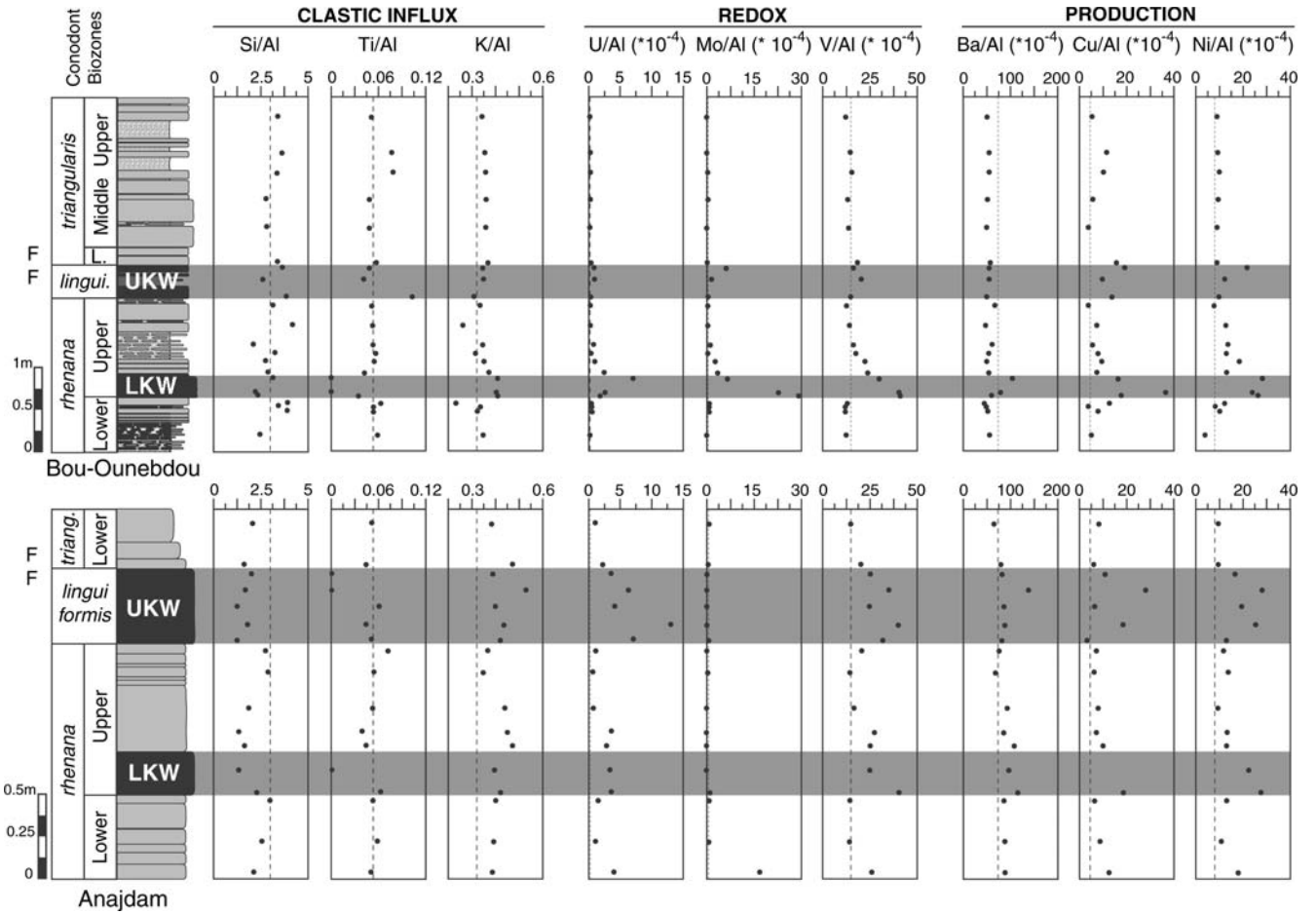

Fig. 8. Stratigraphical plots of elemental concentrations including proxies for clastic input, redox condition and production for the Anajdam and Bou-Ounebdou sections. Dashed lines indicate the metal/aluminium concentration ratios for average shales (Wedepohl 1971, 1991).

Palaeoredox proxies. In each section studied, a significant feature of the F–F boundary sequence is a remarkable enrichment in Mo, U and V in the KW horizons compared to the concentrations in the overlying and underlying strata (Fig. 8). These elements are thought to be redox-sensitive (Calvert & Pedersen 1993; Crusius *et al.* 1996; Dean *et al.* 1997; Algeo & Maynard 2004). The high ratios of these elements in the KW horizons thus suggest that the sediments were probably O_2-deficient. To confirm these observations, V/Cr, V/(V + Ni), U/Th and Ni/Co ratios, which are considered as reliable redox indexes (Hatch & Leventhal 1992; Jones & Manning 1994), were calculated in order to show the contrasted values between the KW horizons and the other parts of the section and to estimate the level of oxygenation (Fig. 9a–d). For each of the indexes used, two clusters of values can be identified, one corresponding to the samples from the KW horizons, the other corresponding to the samples from the overlying and underlying strata. The samples from the KW horizons show the highest values. They are broadly characterized by values of V/Cr > 1.5; U/Th > 1.5; Ni/Co > 4.25 (Fig. 9a, b and d). The values of the V/(V + Ni) ratios are mainly comprised between 0.5 and 0.7 and do not allow clearly distinguishing the KW horizons from the rest of the section (Fig. 9c).

Palaeoproductivity proxies. Vertical concentration profiles of Ba, Cu and Ni to Al ratios indicate slight enrichment in the KW horizons (Fig. 8). In

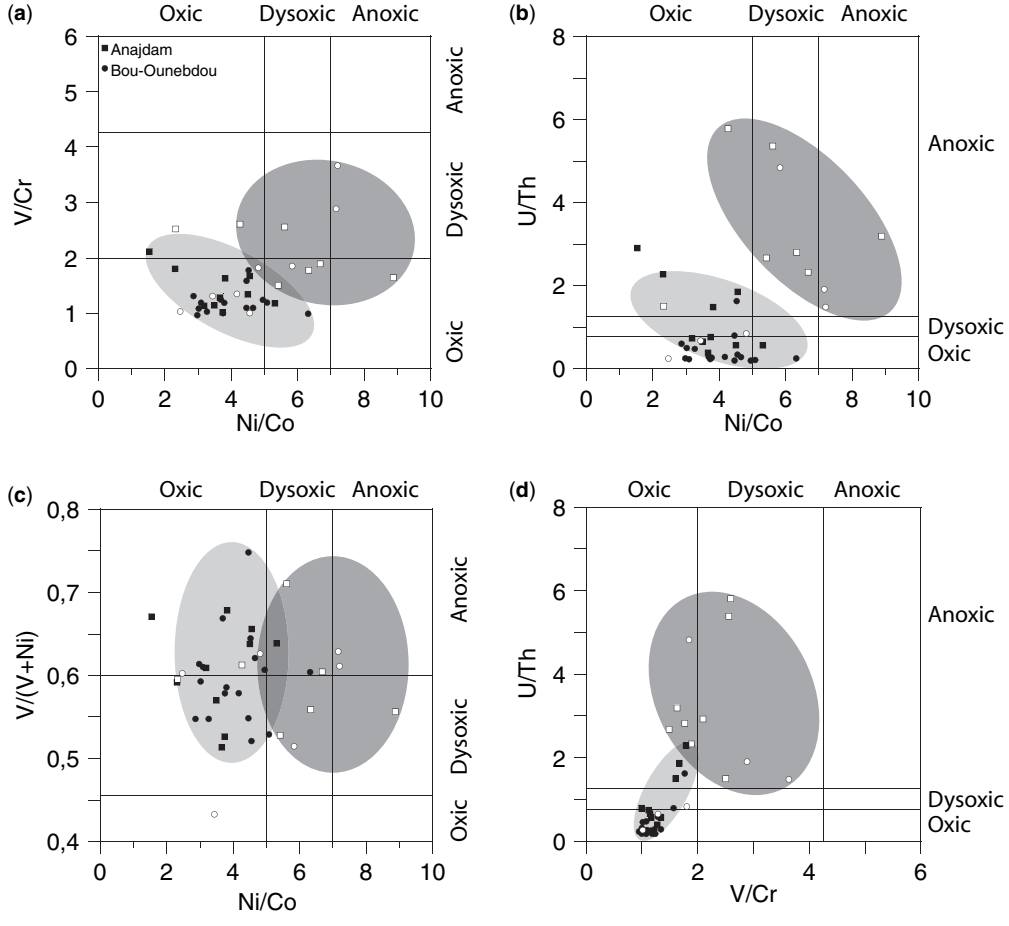

Fig. 9. Crossplots of trace-elements ratios used as palaeoredox proxies. (**a**) V/Cr *vs.* Ni/Co, (**b**) V/(V + Ni) *vs.* Ni/Co, (**c**) U/Th *vs.* Ni/Co and (**d**) U/Th *vs.* V/Cr. Ranges for V/Cr, U/Th and Ni/Co are from Jones & Manning (1994); ranges for V/(V + Ni) are from Hatch & Leventhal (1992). Open symbols: Kellwasser samples.

both sections, most of the KW samples show values of $Cu/Al > 10$ and $Ni/Al > 15$. Ba/Al ratios are higher in Anajdam ($Ba/Al > 90$) than in Bou-Ounebdou ($Ba/Al > 60$) in the KW horizons. Ba abundance is commonly used as a palaeoproductivity marker even if the interpretation is not always straightforward because barite can be dissolved in case of intense sulphate-reduction (McManus *et al.* 1998). In that case, Ba can be released to pore waters, migrate with them, and then reprecipitate when less-reducing conditions are met. Thus barite migration fronts may form (e.g. McManus *et al.* 1998). In the present case, the redox proxies indicate that depositional conditions were probably not very reducing (except for the LKW at Bou-Ounebdou). Consequently, Ba distribution must not have been deeply altered by diagenetical remobilization. The distribution of dissolved Ni and Cu in the ocean appears to be related to settling organic debris, since Ni and Cu behave as micronutrients (Calvert & Pedersen 1993; Algeo & Maynard 2004). These elements are readily adsorbed onto organic particles settling through the water column. So, decaying organic matter (OM) easily forms organometal complexes that can be incorporated into the sediment (Algeo & Maynard 2004; Tribovillard *et al.* 2004*b*). Thus, these elements are usually trapped with organic particles and are incorporated into iron sulphides during diagenesis. Consequently, they are preserved in the sediment even in the case of complete OM remineralization as well as in the case of marked thermal evolution (Mongenot *et al.* 1996). Thus, Ni and Cu may serve as indicators of organic inputs (Tribovillard *et al.* 2000, 2004*b*).

Summary. The distribution of the geochemical data during the Late Devonian suggests that: (1) the KW horizons coincide with two periods of relative decline of detrital influx, marked by a decrease of Ti and Si concentration; (2) the moderate and limited increase of U, Mo and V, as well as Ba, Cu and Ni concentrations are indicators of periods of dysoxic to anoxic conditions and enhanced productivity, that probably caused an increase of OM deposition.

Discussion

Detrital input versus carbonate production in the Frasnian–Famennian times in central Morocco

As previously mentioned, the χ measurements can be used as a good indicator of detrital input in ancient sedimentary rocks if not strongly altered by diagenetic or weathering processes (e.g. Ellwood *et al.* 2000). In the Bou-Ounebdou section, the χ signal is thought to have been modified by weathering processes and goethite formation and, therefore, cannot be considered to decipher detrital supply variations. By contrast, in Anajdam, magnetite and clays are the main minerals controlling the χ signal. This section is thus potentially adequate for relating the detrital input evolution through the F–F times. The possible impact of diagenesis on the magnetic signal still remains to be discussed. As shown by clay mineralogical assemblages, the two sections have been affected by a pronounced diagenesis. In such conditions, the transformation of clays of smectite type into illite has been suggested to induce the formation of authigenic magnetite that can potentially overprint or at least alter the primary detrital magnetic signal (e.g. Katz *et al.* 2000; Zegers *et al.* 2003). As observed in the Day-Fuller plot (Fig. 6c), the distribution of samples from Anajdam cluster below the line established by Channell & McCabe (1994) for diagenesis-induced remagnetized limestones (Fig. 6c).

Therefore, the primary depositional ferromagnetic signal is likely to have not been completely overprinted by diagenetic processes. Furthermore, M_s, that provides a first-order quantitative estimate of the magnetite concentration, does not correlate with either the illite crystallinity index standard or with the illite percentage (Fig. 10a, b). A slight negative correlation can be roughly observed between M_s and the illite percentage, suggesting that the diagenesis-induced illitization is not accompanied by an increase in the magnetite concentration. On the other hand, early diagenetic reductive dissolution of magnetite in the OM-bearing black KW carbonate levels cannot be proposed as an efficient process in the alteration of the primary magnetic signal (e.g. Machel 1995; Robinson *et al.* 2000; Tribovillard *et al.* 2002, 2004*b*), because the high field SC is strongly diamagnetic (Fig. 6c) and thus does not record any effects of authigenic paramagnetic pyrite. Such a poor control of diagenetic processes upon the magnetic signal is corroborated by the correlation of Ti and Th contents ($r^2 = 0.47$ and 0.66, respectively), classically considered as detrital indicators independent of diagenesis-induced remobilization, with the magnetic susceptibility from the Anajdam section (Fig. 11a, b). These whole data thus demonstrate that, although submitted to significant burial, the χ signal can be confidently used as an indicator of the detrital input evolution in the Anajdam section.

The long-term decrease of χ observed during most of the Frasnian times can thus be interpreted

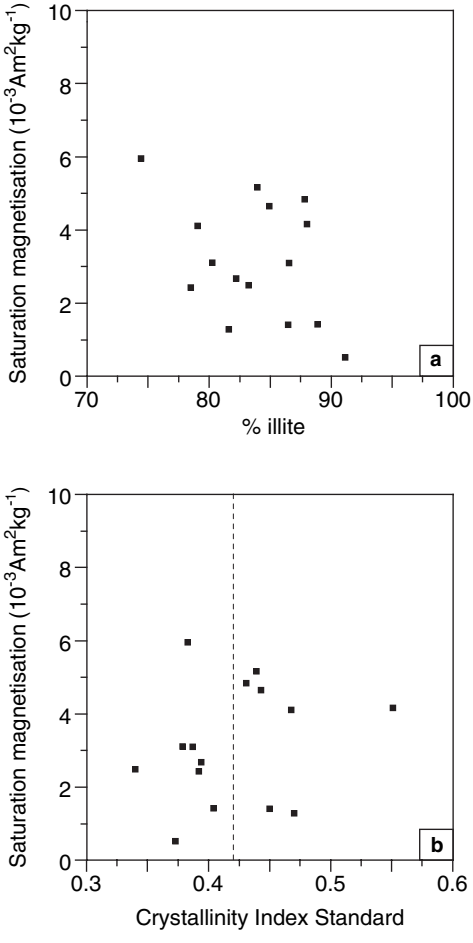

Fig. 10. Hysteresis parameters plotted against clay parameters for representative samples from Anajdam and Bou-Ounebdou. (**a**) Saturation magnetization (M_s) *vs.* CIS. (**b**) Saturation magnetization (M_s) *vs.* % of illite.

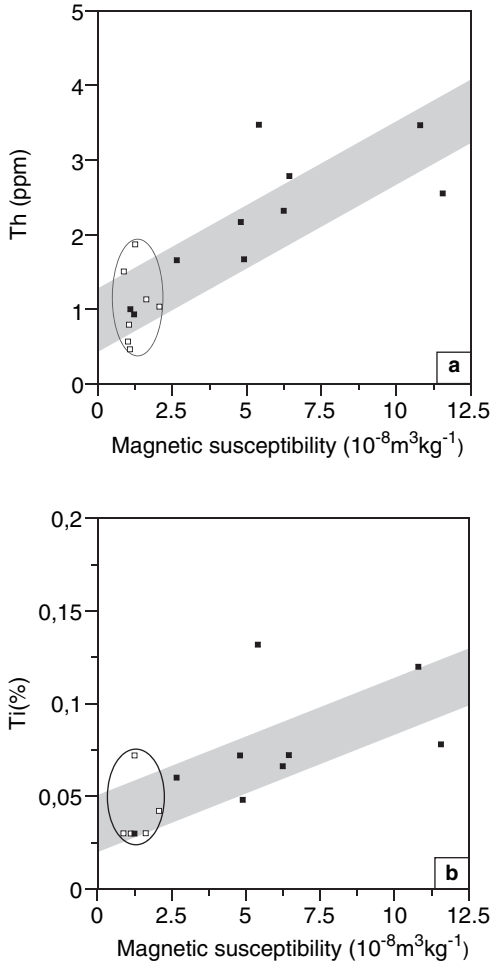

Fig. 11. Detrital-derived element concentrations plotted against low-field magnetic susceptibility (χ) for representative samples from Anajdam. (**a**) Th (ppm) *vs.* χ and (**b**) Ti (%) *vs.* χ.

as a general diminution of the detrital input in the Azrou–Kenifra Basin through Late Frasnian times. This evolution can be traced up to the KW levels that record the lowest χ values, in relation with a minimum detrital input and an enhanced carbonate productivity, as shown by the maximum intensity of the diamagnetic contribution. This is also confirmed by the vertical distribution of Ti/Al and Si/Al ratios related to clastic input (Fig. 8). The F–F boundary represents a significant break in this long-term evolution with a significant increase of the χ, thus suggesting a noticeable increase of the basinal detrital supply. It is worth noting that these variations can be paralleled to the global sea-level fluctuations as synthesized by Sandberg *et al.* (2002) and indicating a general Frasnian sea-level rise, a Late Frasnian highstand, and a F–F boundary sea-level fall (Fig. 12). These sea-level changes have been well documented in several areas, such as Germany (Piecha 2002; Devleeschouwer *et al.* 2002), Poland (Racki *et al.* 2002), NW Australia (Becker & House 1997), China (Chen & Tucker 2003, 2004), and Canada (Mountjoy & Becker 2000).

In a more general perspective, the magnetic susceptibility data from Anajdam are consistent with previous magnetic results obtained from other sections of the northern Gondwana

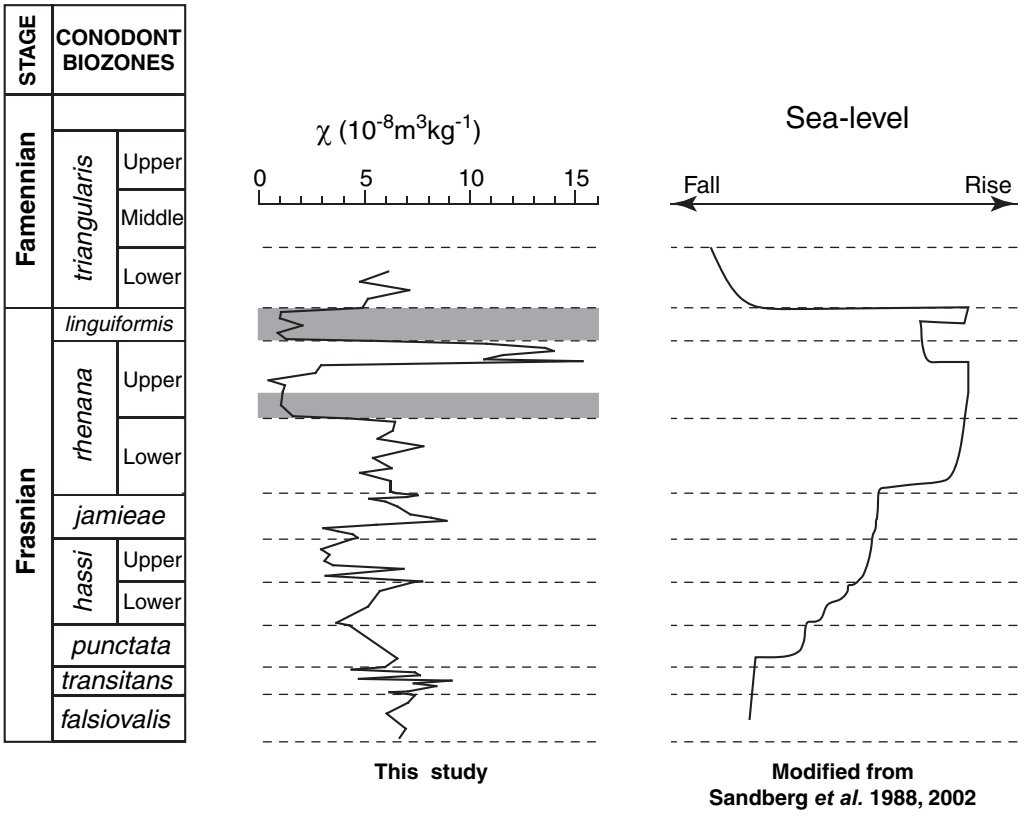

Fig. 12. Synthetic diagram showing the variations of the χ signal obtained from the Anajdam section compared with the Late Devonian sea-level curve (modified from Sandberg *et al.* 1988, 2002).

margin, such as Coumiac (Montagne Noire, S. France), but also from domains of the southern Laurassian margin, such as Steinbruch Schmidt and Beringhausen Tunnel (Rhenish Massif, Germany), Kowala (Holly Cross Mountains, Poland) or Sinsin (Ardennes, Belgium) (Devleeschouwer 1999; Crick *et al.* 2002; Racki *et al.* 2002; Averbuch *et al.* 2005). The mechanisms controlling the first-order observed χ variations have thus to be found in relatively large-scale processes affecting at least the Gondwanan and Laurassian margins. Global climatic warming during Frasnian times with maximum temperatures in the Late Frasnian (Kellwasser events) and global cooling at the F–F boundary are thus the more convincing parameters to account for the observed variations as also suggested by the $\delta^{18}O$ signatures of marine conodont apatite (Joachimski & Buggisch 2002; Joachimski *et al.* 2004) and the miospore diversity evolution on continents (Streel *et al.* 2000).

Marine bottom-water redox-conditions and primary productivity evolution

As mentioned in the 'Results' section, the black limestones of the KW horizons show noticeable variations for nearly all trace element ratios compared to the underlying and overlying limestone beds. Broadly, redox-sensitive elements as well as redox indexes show enrichments in the LKW horizon in Bou-Ounebdou and in the UKW horizon in Anajdam (Fig. 8). Molybdenum concentration has been suggested to be enhanced in the presence of sulphides (Helz *et al.* 1996; Adelson *et al.* 2001; Zheng *et al.* 2000; Vorlicek & Helz 2002; Lyons *et al.* 2003; Algeo & Maynard 2004; Rimmer *et al.* 2004; Tribovillard *et al.* 2004*c*). The marked Mo enrichment observed in the LKW of the Bou-Ounebdou section argues for sulphidic conditions, whereas in all the other parts of the two sections studied, dysoxic–anoxic conditions are put forward (no Mo-enrichment but

relative enrichment in U and V for the KW horizons).

The depletion in O_2 is confirmed by the stratigraphical variations of reliable palaeo-oxygenation indexes such as V/Cr, V/(V + Ni), U/Th, Ni/Co (Fig. 9a–d). In this study, we adopted thresholds proposed by Jones & Manning (1994) and Hatch & Leventhal (1992). For each of the indices used, values indicate anoxic to dysoxic conditions for the two KW horizons. The observed enrichments in redox-sensitive trace elements confirm that the oxic–anoxic interface was located at a shallower depth in the sediment during the deposition of the KW horizons, perhaps even in the water column for the LKW at Bou-Ounebdou. However, the intensity of O_2 depletion is interpreted differently from one ratio to the other (Fig. 9a–d). According to V/Cr and V/(V + Ni) ratios, Late Frasnian conditions were broadly dysoxic to anoxic in outer platform settings, whereas O_2-depletion would be only limited to the KW horizons according to U/Th and Ni/Co. The consistency of the chemical data thus clearly indicates two pulses of oxygen depletion near the base of the Upper *rhenana* Zone and in the *linguiformis* Zone, i.e. within the two KW horizons.

These geochemical results are in agreement with recent biofacies studies (Lazreq 1999; Feist 2002), which demonstrated that in the M'rirt area, the fauna of KW horizons are characterized by a lack of endobenthos and O_2-sensitive epibenthos, such as trilobites and brachiopods. In a more global pattern, our interpretations are in agreement with recent geochemical studies concerning some F–F sections from Germany, France, Poland, Siberia and China (e.g. Racki *et al.* 2002; Ma & Bai 2002; Yudina *et al.* 2002; Bond *et al.* 2004; Tribovillard *et al.* 2004*a*; Pujol *et al.* in press). In many areas, the F–F boundary records some elemental anomalies related to redox conditions (e.g. U, V and Mo). Thus, both geochemical and palaeontological analyses suggest a noticeable decrease of O_2 concentration in bottom waters during the two KW episodes. Primary productivity tracers such as Ba/Al and OM-related elemental ratios, such as Ni/Al and Cu/Al, display a consistent slight increase through the KW levels. A similar trend is also observed in the carbonate production as shown both by the $CaCO_3$ content and the optimal diamagnetic contribution to the magnetic signal. Trends similar to those observed for the Moroccan sections have been found in the time-equivalent formations of Aeketal (Harz, Germany), along the southern Laurassian outer shelf (Riquier *et al.* 2005). Compared to geochemical results obtained for deeper sections such as La Serre (Montagne Noire, France; Tribovillard *et al.* 2004*a*), the Moroccan sections display a relatively low enrichment in Ba. According to Bishop (1988), precipitation of barite is favoured in microenvironments, where OM decays from surface water to sea floor. Therefore, barite may not be enriched in shallow, highly productive environments, whereas it is enhanced in deeper sites with similar productivity. The relatively poor record of primary productivity in outer shelves can thus be explained by local conditions. In shallow-water settings, even if conditions become eutrophic, favouring the onset of O_2-deprived conditions, generally intense seawater mixing does not allow a good preservation of OM. Organic elements are remineralized before reaching the water/sediment interface. The observed enrichments in productivity indicators are coeval with two positive excursions of the carbon isotopic signal ($\delta^{13}C_{carb} = +3‰$ V-PDB), recorded in Bou-Ounebdou and in many other F–F sections for inorganic carbon (Joachimski *et al.* 2002). These positive shifts in $\delta^{13}C$ are explained by an increase in the global-scale organic carbon burial rate in the Late Frasnian seas (Joachimski *et al.* 2001, 2002; Murphy *et al.* 2000*a*, *b*). In outer shelf settings such as the Moroccan sections, the resultant depletion in marine bottom-water oxygenation and associated OM preservation were probably moderate due to efficient platform ventilation.

Conclusion

In this study, rock magnetic measurements (magnetic susceptibility and hysteresis), combined with clay mineral and geochemical analyses allow to constrain the environmental features of two sections from Central Morocco (Anajdam and Bou-Ounebdou). Although both sections were affected by a pronounced diagenesis (limit of anchizonal conditions), we demonstrate that the magnetic susceptibility represents a semi-quantitative proxy for detrital supply variations. The magnetic signal in the Anajdam section is better defined than that in Bou-Ounebdou, owing to increasing weathering intensity in the latter and transformation of high-susceptibility magnetite into low-susceptibility goethite. The Anajdam section unravels a Frasnian long-term decrease of the basinal detrital input that parallels a general sea-level rise with a major highstand in the Late Frasnian Kellwasser-type levels. The Kellwasser Horizons display the lowest values of magnetic susceptibility and magnetization at saturation, in relation with a minimum detrital input and a maximum carbonate productivity, as shown by the significant diamagnetic contribution to the magnetic signal. The high marine primary productivity in the Late-Frasnian Central Moroccan basin is attested by an increase

of the Ba/Al ratio in the Kellwasser levels of both sections. Reliable redox indicators such as V/Cr or U/Th furthermore evidence the general dysoxic conditions prevailing in marine bottom-waters at that time. On top of the Upper Kellwasser Horizon, the Frasnian–Famennian boundary in central Morocco is marked by a break in the sedimentation with possible depositional hiatuses associated with a noticeable sea-level fall (Lazreq 1999; Chakiri 2002). Comparisons with other sections worldwide suggest that the variations in the detrital supply are climatically driven, thus arguing for a long-term Frasnian warming and a significant basal Famennian global cooling event. The latter is subsequent to a Late Frasnian climatic optima leading to a period of particularly increased organic carbon burial (e.g. Joachimski *et al.* 2002). As previously proposed by different authors (e.g. Becker & House 1994; Godderis & Joachimski 2004; Averbuch *et al.* 2005), this mechanism would have produced an important drawdown in the atmospheric CO_2 content, thus resulting in a strong reduction of greenhouse effects in Famennian times. Such rapid variations in seawater oxygenation conditions and temperatures are likely to have had drastic repercussions on marine fauna, potentially leading to the Frasnian–Famennian biological crisis.

This study has been financially supported by the Eclipse program of the C.N.R.S. (project Frasnian–Famennian boundary crisis, O. Averbuch coordinator) and is a contribution of the UMR PBDS 8110. We greatly thank C. Kissel for providing access to the Micromag equipment at the Palaeomagnetic Laboratory in LSCE (Gif sur Yvette), J. Morel for the ICP analyses and M. Frere, P. Recourt and D. Malengros for assistance with X-ray analysis. A. Herbosch, I. Berra and C. Crônier are acknowledged for their participation to the sampling field-trip in Central Morocco. We also thank Michael Joachimski, Grzegorz Racki and Walter Dean for scientific discussions at earlier stages of this study. Finally, we are grateful to Eberhard Schindler and Thomas Becker; the manuscript benefited from their helpful and constructive comments.

References

ADELSON, J. M., HELZ, G. R. & MILLER, C. V. 2001. Reconstructing the rise of recent coastal anoxia; molybdenum in Chesapeake Bay sediments. *Geochimica Cosmochimica Acta*, **65**, 237–252.

ALGEO, T. J. & SCHECKLER, S. E. 1998. Terrestrial–marine teleconnections in the Devonian: links between the evolution of land plants, weathering processes, and marine anoxic events. *Philosophical Transactions of the Royal Society of London*, **B353**, 113–130.

ALGEO, T. J. & MAYNARD, J. B. 2004. Trace element behavior and redox facies analysis of core shales of Upper Pennsylvanian Kansas-type cyclotherms. *Chemical Geology*, **206**, 289–318.

AVERBUCH, O., TRIBOVILLARD, N., DEVLEESCHOUWER, X., RIQUIER, L., MISTIAEN, B. & VAN VLIET-LANOE, B. 2005. Mountain building—enhanced continental weathering and organic carbon burial as major causes for climatic cooling at the Frasnian–Famennian boundary (ca 376 Ma BP). *Terra Nova*, **17**, 25–34.

BECKER, R. T. 1993. Stratigraphische Gliederung und Ammonoideen-Faunen im Nehdenium (Oberdevon II) von Europa und Nord-Afrika. *Courier Forschungsinstitut Senckenberg*, **155**, 1–405.

BECKER, R. T. & HOUSE, M. R. 1994. Kellwasser Events and goniatite successions in the Devonian of the Montagne Noire with comments on possible causations. *Courier Forschungsinstitut Senckenberg*, **169**, 45–77.

BECKER, R. T. & HOUSE, M. R. 1997. Sea-level changes in the Upper Devonian of the Canning Basin, Western Australia. *Courier Forschunginstitut Senckenberg*, **199**, 129–146.

BECKER, R. T. & HOUSE, M. R. 2000. Sedimentary and faunal succession of the allochtonous Upper Devonian at Gara d'Mrirt (Eastern Moroccan Meseta). *Notes et Mémoires, Service Géologique du Maroc*, **399**, 109–114.

BISHOP, J. K. 1988. The barite-opal-organic carbon association in oceanic particulate matter. *Nature*, **332**, 341–343.

BOND, D., WIGNALL, P. B. & RACKI, G. 2004. Extent and duration of marine anoxia during the Frasnian- Famennian (Late Devonian) mass extinction in Poland, Germany, Austria and France. *Geological Magazine*, **141**, 173–193.

BORRADAILE, G. J., CHOW, N. & WERNET, T. 1993. Magnetic hysteresis of limestones: facies control? *Physics of the Earth and Planetary Interior*, **76**, 241–252.

BOUABDELLI, M. 1989. Tectonique et sédimentation dans un bassin orgénique: le sillon Viséen d'Azrou-Khénifra (Est du Massif Hercynien Central du Maroc). Unpublished Ph.D. thesis, Louis Pasteur University, Strasbourg.

BOUABDELLI, M. & PIQUÉ, A. 1996. Du bassin sur décrochement au basin d'avant-pays: dynamique du bassin d'Azrou-Khénifra (Maroc Hercynien central). *Journal of African Earth Science*, **23**, 213–224.

BRINDLEY, G. W. & BROWN, G. 1980. Crystal structures of clay minerals and their identification. *Mineralogical Society Monograph No. 5*. Mineralogical Society, London.

BUGGISCH, W. 1991. The global Frasnian/Famennian "Kellwasser Event". *Geologische Rundschau*, **80**, 49–72.

BUGGISCH, W. & CLAUSEN, C.-D. 1972. Conodonten- und Goniatiten-Faunen aus dem oberen Frasnium und unteren Famennium Marokkos (Tafilalt, Antiatlas). *Neues Jahrbuch für Geologie und Paläontogie Abhandlungen*, **141**, 137–167.

CALVERT, S. E. & PEDERSEN, T. F. 1993. Geochemistry of Recent oxic and anoxic marine sediments:

Implications for the geological record. *Marine Geology*, **113**, 67–88.

CHAKIRI, S. 2002. Sédimentologie et géodynamique du Maroc Central Hercynien pendant le Dévonien. Unpublished Ph.D. thesis, Ibn Tofail University, Kenitra.

CHANNELL, J. E. T. & MCCABE, C. 1994. Comparison of magnetic hysteresis parameters of unremagnetized and remagnetized limestones. *Journal of Geophysical Research*, **99**, 4613–4623.

CHEN, D. & TUCKER, M. E. 2003. The Frasnian/Famennian mass extinction: insights from high-resolution sequence stratigraphy and cyclostratigraphy in South China. *Palaeogeography, Palaeoclimatology, Palaeoecology*, **193**, 87–111.

CHEN, D. & TUCKER, M. E. 2004. Paleokarst and its implication for the extinction event at the Frasnian-Famennian boundary (Guilin, South China). *Journal of the Geological Society of London*, **161**, 895–898.

COPPER, P. 1986. Frasnian/Famennian mass extinction and cold-water oceans. *Geology*, **14**, 835–839.

CRICK, R. E., ELLWOOD, B. B., HASSANI, A., FIEST, R. & HLADIL, J. 1997. Magnetosusceptibility event and cyclostratigraphy (MSEC) of the Eifelian-Givetian GSSP and associated boundary sequences in North Africa and Europe. *Episodes*, **20**, 167–175.

CRICK, R. E., ELLWOOD, B. B., *ET AL.* 2002. Magneto-stratigraphy susceptibility of the Frasnian/Famennian boundary. *Palaeo-geography, Palaeoclimatology, Palaeoecology*, **181**, 67–90.

CRUSIUS, J., CALVERT, S., PEDERSEN, T. & SAGE, D. 1996. Rhenium and molybdenum enrichments in sediments as indicator of oxic, suboxic and sulfidic conditions of deposition. *Earth and Planetary Sciences Letters*, **145**, 65–78.

DAY, R., FULLER, M. D. & SCHMIDT, V. A. 1977. Hysteresis properties of titanomagnetites. Grain size and composition dependence. *Physics of the Earth and Planetary Interior*, **13**, 260–267.

DEAN, W. E., GARDNER, J. V. & PIPER, D. Z. 1997. Inorganic geochemical indicators of glacial-interglacial changes in productivity and anoxia on the California continental margin. *Geochimica et Cosmochimica Acta*, **61**, 4507–4518.

DEVLEESCHOUWER, X. 1999. La transition Frasnien/Famennien (Dévonien sup.) en Europe: sédimentologie, stratigraphie séquentielle et susceptibilité magnétique. Unpublished Ph.D. thesis, Lille and Brussels Universities.

DEVLEESCHOUWER, X., HERBOSCH, A. & PRÉAT, A. 2002. Microfacies, sequence stratigraphy and clay mineralogy of a condensed deep-water section around the Frasnian–Famennian boundary (Steinbruch Schmidt, Germany). *Palaeoecology, Palaeclimalology, Palaeoecology*, **181**, 171–193.

DOPIERALSKA, J. 2003. Neodymium isotopic composition of conodonts as a palaeoceanographic proxy in the Variscan oceanic system. Unpublished Ph.D. thesis, University of Giessen.

DUNLOP, D. J. 1986. Hysteresis properties of magnetite and their dependence on particle size: a test of pseudo-single domain remanence models. *Journal of Geophysical Research*, **91**, 9569–9584.

EL HASSANI, A. & TAHIRI, A. 2000*a*. The eastern part of central Morocco (western Meseta). *Notes & Mémoires du Service Géologique du Maroc*, **399**, 89–92.

EL HASSANI, A. & TAHIRI, A. (eds) 2000*b*. Moroccan Meeting of the Subcommission on Devonian Stratigraphy (SDS) – IGCP 421 (April 24th–May 1st 1999): Excursion guidebook. *Notes & Mémoires du Service Géologique du Maroc*, **399**, 1–150.

ELLWOOD, B. B., CRICK, R. E., EL HASSANI, A., BENOIST, S. L. & YOUNG, R. H. 2000. Magnetosusceptibility event and cyclostratigraphy method applied to marine rocks: detrital input versus carbonate productivity. *Geology*, **28**, 1135–1138.

FEIST, R. 2002. Trilobites from the latest Frasnian Kellwasser Crisis in North Africa (Mrirt, central Moroccan Meseta). *Acta Palaeontologica Polonica*, **47**, 203–210.

GIRARD, C. & ALBARÈDE, F. 1996. Trace elements in conodont phosphate from the Frasnian/Famennian boundary. *Palaeogeography, Palaeoclimatology, Palaeoecology*, **126**, 195–209.

GIRARD, C., KLAPPER, G. & FEIST, R. 2005. Subdivision of the terminal Frasnian *linguiformis* conodont Zone, revision of the correlative interval of Montagne Noire Zone 13, and discussion of stratigraphically significant associated trilobites. *In*: OVER, J., MORROW, J. R. & WIGNALL, P. (eds) *Understanding Late Devonian Triassic Biotic and Climatic Events; Towards an Integrated Approach*, 181–198.

GODDERIS, Y. & JOACHIMSKI, M. M. 2004. Global change in the Late Devonian: Modelling the Frasnian-Famennian short-term carbone isotope excursions. *Palaeogeography, Palaeoclimatology Palaeoecology*, **202**, 309–329.

GRADSTEIN, F. M., OGG, J. G. *ET AL.* 2004. *A Geologic Time Scale 2004*. Cambridge University Press.

HALLAM, A. & WIGNALL, P. B. 1999. Mass extinctions and sea-level changes. *Earth Science Reviews*, **48**, 217–250.

HATCH, J. R. & LEVENTHAL, J. S. 1992. Relationship between inferred redox potential of the depositional environment and geochemistry of the Upper Pennsylvanian (Missourian) Stark Shale Member of the Dennis Limestone, Wabaunsee County, Kansas, U.S.A. *Chemical Geology*, **99**, 65–82.

HELLER, F. 1978. Rock magnetic studies of Upper Jurassic limestones from Southern Germany. *Zeitschrift für Geophysik*, **44**, 525–543.

HELZ, G. R., MILLER, C. V., CHARNOCK, J. M., MOSSELMANS, J. L. W., PATTRICK, R. A. D., GARNER, C. D. & VAUGHAN, D. J. 1996. Mechanisms of molybdenum removal from the sea and its concentration in black shales: EXAFS evidences. *Geochimica Cosmochimica Acta*, **60**, 3631–3642.

HOLTZAPFFEL, T. 1985. Les minéraux argileux. Préparation, analyse diffractométrique et détermination. *Mémoire Société Géologique du Nord*, **12**, 136pp.

HOUSE, M. R. 2002. Strength, timing, setting and cause of mid-Palaeozoic extinctions. *Palaeogeography, Palaeoclimatology, Palaeoecology*, **181**, 5–25.

JOACHIMSKI, M. M. & BUGGISCH, W. 1993. Anoxic events in the Late Frasnian—causes of the Frasnian–Famennian faunal crisis? *Geology*, **21**, 675–678.

JOACHIMSKI, M. M. & BUGGISCH, W. 2002. Conodont apatite $\delta^{18}O$ signatures indicate climatic cooling as a trigger of the Late Devonian mass extinction. *Geology*, **30**, 711–714.

JOACHIMSKI, M. M., OSTERTAG-HENNING, C., *ET AL.* 2001. Water column anoxia, enhanced productivity and concomitant changes in $\delta^{13}C$ and $\delta^{34}S$ across the Frasnian–Famennian boundary (Kowala—Holy Cross Mountains/Poland). *Chemical Geology*, **175**, 109–131.

JOACHIMSKI, M. M., PANCOST, R. D., FREEMAN, K. H., OSTERTAG-HENNING, C. & BUGGISCH, W. 2002. Carbon isotope geochemistry of the Frasnian-Famennian transition. *Palaeogeography, Palaeoclimatology, Palaeoecology*, **181**, 91–109.

JOACHIMSKI, M. M., VAN GELDERN, R., BREISIG, S., BUGGISCH, W. & DAY, J. 2004. Oxygen isotope evolution of biogenic calcite and apatite during the Middle and Late Devonian. *International Journal of Earth Science*, **93**, 542–553.

JONES, B. & MANNING, D. A. C. 1994. Comparison of geochemical indices used for the interpretation of palaeoredox conditions in ancient mudstones. *Chemical Geology*, **111**, 111–129.

KATZ, B., ELMORE, D., COGOINI, M., ENGEL, M. H. & FERRY, S. 2000. Association between burial diagenesis of smectite, chemical remagnetization, and magnetite authigenesis in the Vocontian trough, SE France. *Journal of Geophysical Research*, **105**, 851–868.

LAZREQ, N. 1992. The Upper Devonian of M'rirt (Morocco). *Courier Forschungsinstitut Senckenberg*, **154**, 107–123.

LAZREQ, N. 1999. Biostratigraphie des conodontes du Givétien au Famennien du Maroc Central. Biofaciès et événement Kellwasser. *Courier Forschungsinstitut Senckenberg*, **214**, 1–111.

LYONS, T. W., WERNE, J. P., HOLLANDER, D. J. & MURRAY, R. W. 2003. Contrasting sulfur geochemistry and Fe/Al and Mo/Al ratios across the last oxic-to-anoxic transition in the Cariaco Basin, Venezuela. *Chemical Geology*, **195**, 131–157.

MA, X. P. & BAI, S. L. 2002. Biological, depositional, microspherule, and geochemical records of the Frasnian/Famennian boundary beds, South China. *Palaeogeography, Palaeoclimatology, Palaeo-ecology*, **181**, 325–346.

MCGHEE, G. R. 1996. The Late Devonian Mass Extinction. The Frasnian-Famennian Crisis. Columbia University Press, New York.

MCMANUS, J., BERELSON, W. M., *ET AL.* 1998. Geochemistry of barium in marine sediments: Implications for its use as a paleoproxy. *Geochimica Cosmochimica Acta*, **62**, 3453–3473.

MACHEL, H. 1995. Magnetic mineral assemblages and magnetic contrasts in diagenetic environments—with implications for studies of paleomagnetism, hydrocarbon migration and exploration. *In*: TURNER, P. & TURNER, A. (eds) Paleomagnetic application in hydrocarbon exploration and production. *Geological Society Special Publication*, **98**, 9–29.

MAHER, B. A. & THOMPSON, R. 1999. *Quaternary climates, environments and magnetism*. Cambridge University Press, New York.

MONGENOT, T., TRIBOVILLARD, N.-P., DESPRAIRIES, A., LALLIER-VERGÈS, E. & LAGGOUN-DEFARGE, F. 1996. Trace elements as palaeoenvironmental markers in strongly mature hydrocarbon source rocks: the Cretaceous La Luna Formation of Venezuela. *Sedimentary Geology*, **103**, 23–37.

MOUNTJOY, E. W. & BECKER, S. 2000. Frasnian to Famennian sea-level changes and the Sassenach Formation, Jasper Basin, Alberta Rocky Mountains. *In*: HOMEWOOD, P. W. & EBERLI, G.P. (eds). Genetic stratigraphy on exploration and production shales—Case studies from the Pennsylvanian of the Paradox Basin and the Upper Devonian of Alberta. *Bulletin des Centres de Recherches Elf Exploration Production Memoire*, **24**, 181–201.

MURPHY, A. E., SAGEMAN, B. B. & HOLLANDER, D. J. 2000*a*. Eutrophication by decoupling of the marine geochemical cycles of C, N and P: a mechanism for the Late Devonian mass extinction. *Geology*, **28**, 427–430.

MURPHY, A. E., SAGEMAN, B. B., HOLLANDER, D. J., LYONS, T. L. & BRETT, C. E. 2000*b*. Black shale deposition and faunal overturn in the Devonian Appalachian Basin: clastic starvation, seasonal water-column mixing, and efficient biolimiting nutrient recycling. *Paleoceanography*, **15**, 280–291.

PETSCHICK, R., KUHN, G. & GINGELE, F. 1996. Clay mineral distribution in surface sediments of the South Atlantic: sources, transport, and relation to oceanography. *Marine Geology*, **130**, 203–229.

PIECHA, M. 2002. A considerable hiatus at the Frasnian/Famennian boundary in the Rhenish shelf region of northwest Germany. *Palaeogeography, Palaeoclimatology, Palaeoecology*, **181**, 195–211.

PIQUÉ, A., BOSSIÈRE, G., BOUILLIN, J.-P., CHALOUAN, A. & HOEPFFNER, C. 1993. Southern margin of the Variscan belt: the north-western Gondwana mobile zone (eastern Morocco and northern Algeria). *Geologische Rundschau*, **82**, 432–439.

PUJOL, F., BERNER, Z. & STÜBEN, D. Chemostratigraphy of some european Frasnian-Famennian boundary key section. *Palaeogeography, Palaeoclimatology, Palaeoecology*, **240**, 120–145.

RACKI, G. 1998. Frasnian-Famennian biotic crisis: undervalued tectonic control? *Palaeogeography, Palaeoclimatology, Palaeoecology*, **141**, 177–198.

RACKI, G. 1999. The Frasnian-Famennian biotic crisis: how many (if any) bolide impacts? *Geologische Rundschau*, **87**, 617–632.

RACKI, G., RACKA, M., MATYJA, H. & DEVLEESCOUWER, X. 2002. The Frasnian/Famennian boundary interval in the South Polish–Moravian shelf basins: integrated event-stratigraphical approach. *Palaeogeography, Palaeoclimatology, Palaeoecology*, **181**, 251–297.

RIMMER, S. M., THOMPSON, J. A., GOODNIGHT, S. A. & ROBL, T. L. 2004. Multiple controls on the preservation of organic matter in Devonian–Mississippian marine black shales: geochemical and petrographic evidence. *Palaeogeography, Palaeoclimatology, Palaeoecology*, **215**, 125–154.

RIQUIER, L., TRIBOVILLARD, N., AVERBUCH, O., JOACHIMSKI, M. M., RACKI, G., DEVLEESCHOUWER, X., EL ALBANI, A. & RIBOULLEAU, A. 2005. Bottom water redox conditions at the Frasnian-Famennian boundary on both sides of the Eovariscan Belt constraints from trace element geochemistry. *In*: OVER, J., MORROW, J. R. & WIGNALL, P. (eds) *Understanding Late Devonian and Permian-Triassic Biotic and Climatic Events; Towards an Integrated Approach*, 199–225.

ROBINSON, S. G., SAHOTA, J. T. S. & OLDFIELD, F. 2000. Early diagenesis in North atlantic abyssal plain sediments characterized by rock-magnetic and geochemical indices. *Marine Geology*, **163**, 77–107.

ROBION, P., AVERBUCH, O. & SINTUBIN, M. 1999. Fabric development and metamorphic evolution of Lower Paleozoic slaty rocks from the Rocroi massif (French-Belgian Ardennes): new constraints from magnetic fabrics, phyllosilicate preferred orientation and illite crystallinity data. *Tectonophysics*, **309**, 257–273.

SANDBERG, C. A., ZIEGLER, W., DREESEN, R. & BUTLER, J. L. 1988. Late Frasnian mass extinction: conodont event stratigraphy, global changes, and possible causes. *Courier Forschunginstitut Senckenberg*, **102**, 263–307.

SANDBERG, C. A., MORROW, J. R. & ZIEGLER, W. 2002. Late Devonian sea-level changes, catastrophic events, and mass extinctions. *In*: KOEBERL, C. & MACLEOD, K. G. (eds) Catastrophic Events and Mass Extinctions: Impacts and Beyond: *Geological Society of America Special Paper*, **356**, 473–487.

SCHINDLER, E. 1990. Die Kellwasser Krise (hohe Frasne-Stufe, Ober Devon). *Göttinger Arbeiten zur Geologie und Paläeontologie*, **46**, 1–115.

SEPKOSKI, JR, J. J. 1982. Mass extinctions in the Phanerozoic oceans: A review. *Geological Society of America, Special Papers*, **190**, 283–289.

SEPKOSKI, JR, J. J. 1986. Phanerozoic overview of mass extinctions. *In*: RAUP, D. M. & JABLONSKI, D. (eds) *Patterns and Processes in the History of Life*. Springer-Verlag, Berlin, 277–295.

STREEL, M., CAPUTO, M. V., LOBOZIAK, S. & MELO, J. H. G. 2000. Late Frasnian-Famennian climates based on palynomorph analyses and the question of the Late Devonian glaciations. *Earth-Science Reviews*, **52**, 121–173.

TRIBOVILLARD, N., DUPUIS, C. & ROBIN, E. 2000. Sedimentological and diagenetical conditions of the impact level of the Cretaceous/Tertiary boundary in Tunisia: no anoxia required. *Bulletin de la Société Géologique de France*, **171**, 629–636.

TRIBOVILLARD, N. P., DESPRAIRIES, A., LALLIER-VERGES, E., BERTRAND, P., MOUREAU, N., RAMDANI, A. & RAMANAMPOSOA, L. 1994. Geochemical study of organic-matter rich cycles from the Kimmeridge clay formation of Yorkshire (UK): productivity versus anoxia. *Palaeogeography, Palaeoclimatology, Palaeoecology*, **108**, 165–181.

TRIBOVILLARD, N., AVERBUCH, O., BIALKOWSKI, A. & DECONINCK, J.-F. 2002. The influence of early diagenesis of marine organic matter on the magnetic susceptibility signal of sedimentary rocks. *Bulletin de la Société Géologique de France*, **172**, 295–306.

TRIBOVILLARD, N., AVERBUCH, O., DEVLEESCHOUWER, X., RACKI, G. & RIBOULLEAU, A. 2004*a*. Deep-water anoxia over the Frasnian-Famennian boundary (La Serre, France): a tectonically induced oceanic anoxic event? *Terra Nova*, **16**, 288–295.

TRIBOVILLARD, N., AVERBUCH, O. & RIBOULLEAU, A. 2004*b*. Influence of marine organic-matter diagenesis on magnetic susceptibility of sedimentary rocks: the sulphide pathway. *Annales de la Société Géologique du Nord*, **11**, 57–67.

TRIBOVILLARD, N., RIBOULLEAU, A., LYONS, T. & BAUDIN, F. 2004*c*. Enhanced trapping of molybdenum by sulfurized marine organic matter of origin in Mesozoic limestones and shales. *Chemical Geology*, **213**, 385–401.

VANDERAVEROET, P., AVERBUCH, O., DECONINCK, J.-F. & CHAMLEY, H. 1999. Glacial/interglacial cycles in Pleistocene sediments of New Jersey expressed by clay minerals, grain-size and magnetic susceptibility data. *Marine Geology*, **159**, 79–92.

VORLICEK, T. P. & HELZ, G. R. 2002. Catalysis by mineral surfaces: implications for Mo geochemistry in anoxic environments. *Geochimica Cosmochimica Acta*, **66**, 3679–3692.

WALDEN, J., OLDFIELD, F. & SMITH, J. 1999. Environmental magnetism: a practical guide. *Technical Guide No. 6*, Quaternary Research Association, London, 243pp.

WALLISER, O. H. 1996. *Global events and event stratigraphy in the Phanerozoic: Results of international interdisciplinary cooperation in the IGCP Project 216 "Global Biological Events in Earth History"*. Springer-Verlag, Heidelberg.

WALLISER, O. H., EL HASSANI, H. & TAHIRI, A. 2000. M'rirt: a key area for the Variscan Meseta of Morocco. *Notes et Mémoires, Service Géologique du Maroc*, **399**, 93–108.

WARR, L. N. & RICE, A. H. 1994. Interlaboratory standardization and calibration of clay mineral crystallinity and crystallite size data. *Journal of Metamorphic Geology*, **12**, 141–152.

WEDEPOHL, K. H. 1971. Environmental influences on the chemical composition of shales and clays. *In*: AHRENS, L. H., PRESS, F., RUNCORN, S. K. & UREY, H. C. (eds) *Physics and Chemistry of the Earth*, Pergamon, Oxford, pp. 305–333.

WEDEPOHL, K. H. 1991. The composition of the upper Earth's crust and the natural cycles of selected metals. *In*: MERIAN, E. (eds) *Metals and their compounds in the Environment*, VCH-Verlagsgesel lschaft, Weinheim, pp. 3–17.

WENDT, J. & BELKA, Z. 1991. Age and depositional environment of Upper Devonian (Early Frasnian to Early Famennian) black shales and limestones (Kellwasser Facies) in the Eastern Anti-Atlas, Morocco. *Facies*, **25**, 51–90.

YUDINA, A. B., RACKI, G., SAVAGE, N. S., RACKA, M. & MALKOWSKI, K. 2002. The Frasnian-Famennian events in deep-shelf succession, Subpolar Urals: biotic, depositional and geochemical records. *Acta Palaeontologica Polonica*, **47**, 355–372.

ZEGERS, T. E., DEKKERS, M. J. & BAILLY, S. 2003. Late Carboniferous to Permian remagnetization of Devonian limestones in the Ardennes: role of temperature, fluids, and deformation. *Journal of Geophysical Research*, **108**, 2357.

ZHENG, Y., ANDERSON, R. F., VAN GEEN, A. & KUWABARA, J. 2000. Authigenic molybdenum formation in marine sediments: a link to pore water sulfide in the Santa Barbara Basin. *Geochimica Cosmochimica Acta*, **64**, 4165–4178.